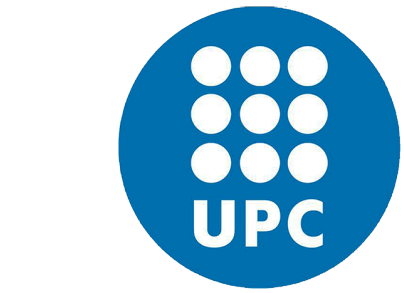

UNIVERSITAT POLITÈCNICA
DE CATALUNYA
BARCELONATECH

Small-Signal Stability Studies under Converter-Based Generator Replacement: Modal Analysis of VSC Integration in Hydro-Dominated Benchmark Grids - IEEE Brazilian 7-Bus System

Joseph Usman
joseph.usman@estudiantat.upc.edu

Stephanie Matta
stephanie.mattabobadilla@estudiantat.upc.edu

Supervised by: **Prof. Marc Cheah Mañe**

June 29, 2025

Escola Tècnica Superior
d'Enginyeria Industrial de Barcelona

Contents

Abstract

This study provides a comprehensive small-signal stability assessment of a hydro-dominated, 7-bus power system as synchronous generation is progressively replaced by grid-following voltage-source converters (VSCs). While the energy transition for renewable-based power systems promises lower carbon emissions and greater operational flexibility, it also challenges old assumptions about grid dynamics, particularly concerning system inertia, fault-current contributions, and the nature of small-signal oscillatory modes, since the nowadays conversation turns around a lower inertia system based on renewables, this study focus con control enhancement and tuning for increasing the stability margins of each variation made in the simulations, being a main goal to operate withe the widest range of stability. Building on a validated base case with five large hydro units. We first stabilized the unstable system by tuning the gain of the Exciter. Then we examined two replacement scenarios, substituting one and then two synchronous machines with Grid following VSCs employing the STAMP toolbox to automatically generate linear state-space and nonlinear EMT models in all the cases. In each scenario, we conducted eigenvalue-based modal analysis to identify shifts in oscillation frequencies, damping ratios, and modal participation. Our findings reveal that the system also exhibit inter-area oscillations as seen in the dynamics presented in the participation matrix and modal analysis. As a result, even a single VSC swap triggers the emergence of six unstable or lightly damped modes: high frequency resonances were tied to the converter's filter and switching dynamics, and low frequency electromechanical swings among the remaining synchronous machines. Replacing two generators had similar effects, that is, significantly reduced system's inertia and modal separation. We then explore control loop tuning options, demonstrating that aggressive current controller gains have limited impact, whereas modest increases in the outer power loop time constant τ_{pq} in both scenario effectively reassign all modes into the left half-plane. Overall, this work highlights the critical role of inertia, tailored power loop dynamics, and active damping strategies in ensuring stable, low inertia grids with high converter penetration. These insights provide practical guidelines for controller design and system planning in renewable energy integration.

1 Introduction

What would happen if water resources were no longer available for electricity generation? Today, hydropower is becoming increasingly critical due to climate change, industrial overuse, and competing demands for sanitation and agriculture. In several countries, hydropower plants have been partially shut down in times of crisis to prioritize human and environmental needs over electricity generation.

In the REmap analysis for Central America presented by IRENA[1], the decarbonizing pathway for the region's energy sector has target 82% share of renewables by 2030.

Ensuring secure operation during this transition requires robust tools to assess how new converter-based generation affects system dynamics. In this context, small-signal stability, as defined by Kundur, P.[2] where it refers to the ability of a power system to maintain synchronism when subjected to small perturbations, such as minor load changes or routine switching events, becomes an essential lens to evaluate potential risks of oscillations or loss of synchronism under everyday perturbations.

1.1 Background and Motivation

In regions like South America, where hydroelectricity plays a foundational role in energy planning, this presents a pressing challenge. Brazil's energy mix, for example, currently relies on hydro for approximately 60% of its installed capacity, with renewables representing over 20% as of 2023 [3]. National road-maps target a 45% share of renewables by 2030. This target along with a high energy density, the limitation of water resources, long transmission distances and massive hydro projects existing such as the Itaipu Dam, makes this study fundamental for future grid planning at transmission level.

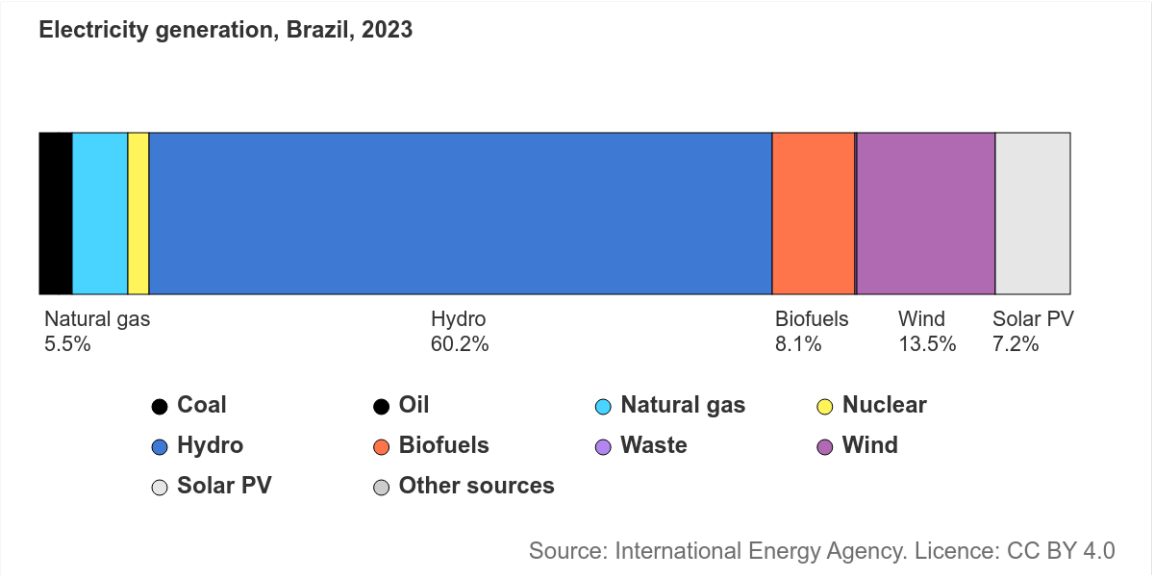

Figure 1: Brazilian Energy Mix 2023.

A key example is the IEEE Brazilian 7-bus benchmark system, where five large hydro plants and their network form a canonical testbed for stability studies[4], a simplified system which captures the general operational dynamics, the topology can be found in Fig.2.

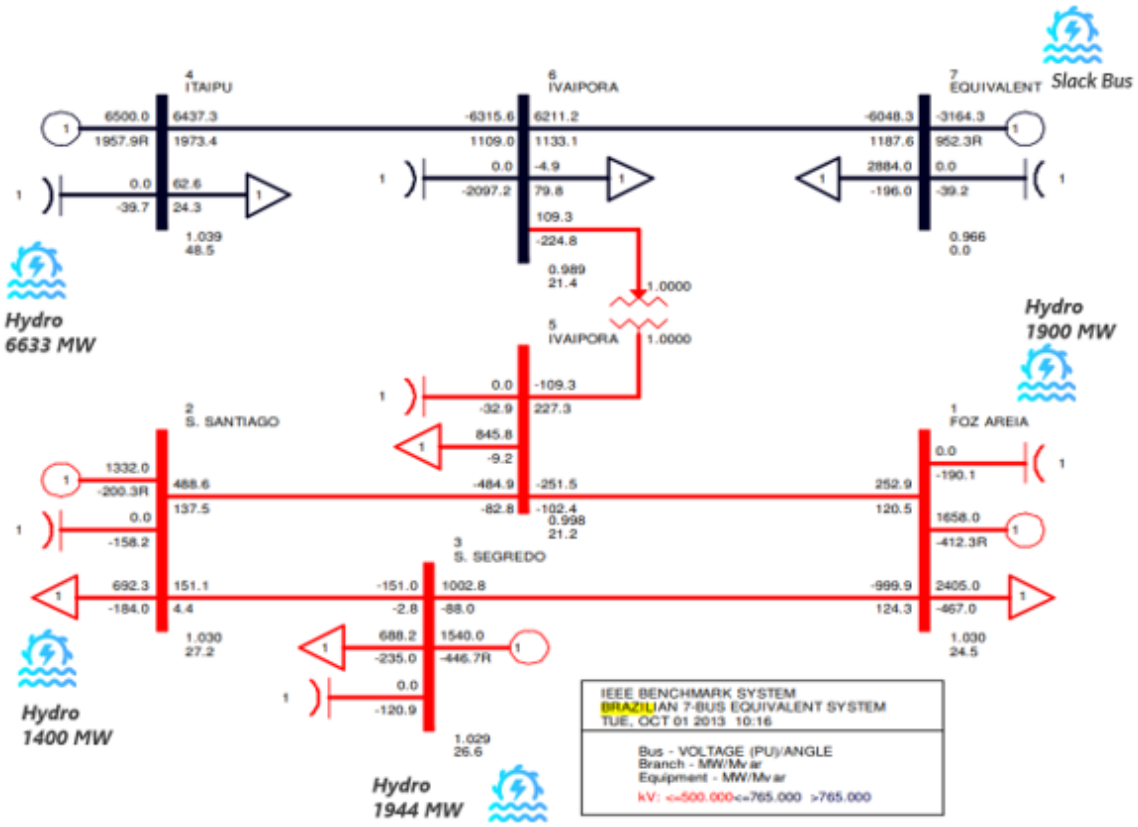

Figure 2: Topology of simulated grid.

In this system, replacing even a fraction of SG power with VSC or HVDC links or large wind farms can dramatically alter modal damping and introduce new poorly damped electromechanical and electromagnetic modes.

Brazil has established itself as a regional leader in HVDC transmission, with a robust network of over five major domestic links, including the Itaipú (1987), Belo Monte (2017), and Madeira (2013) systems, enabling efficient long-distance power delivery from remote hydropower plants to key demand centers. While the country actively explores cross-border energy integration, its existing interconnections with neighboring nations (Argentina, Uruguay, Paraguay, and Bolivia) currently rely on AC technology. Brazil's continued investments in HV infrastructure and testing underscore its pivotal role in advancing grid modernization and supporting South America's energy transition.

1.2 STAMP Tool

The targeted small-signal studies were conducted using the open source STAMP Toolbox, a MATLAB-based framework designed to automate small-signal stability analysis and generate electromagnetic transient (EMT) models of power systems, designed by Universitat Politecnica

de Catalunya and the Research Center CITCEA-UPC.

The use of STAMP tool enables detailed modeling of converter-dominated networks, combining both frequency-domain and time-domain analysis, constructing linearized models for eigenvalue analysis and nonlinear models in Simulink for time-domain validation, which is particularly useful when evaluating medium to large power systems and its dynamic interactions.

Parameters from the Brazilian Network System [4] were loaded into the tool through excel-based worksheets for its linearization and state space models. The STAMP tool logic for data-processing and model is shown in Fig.3.

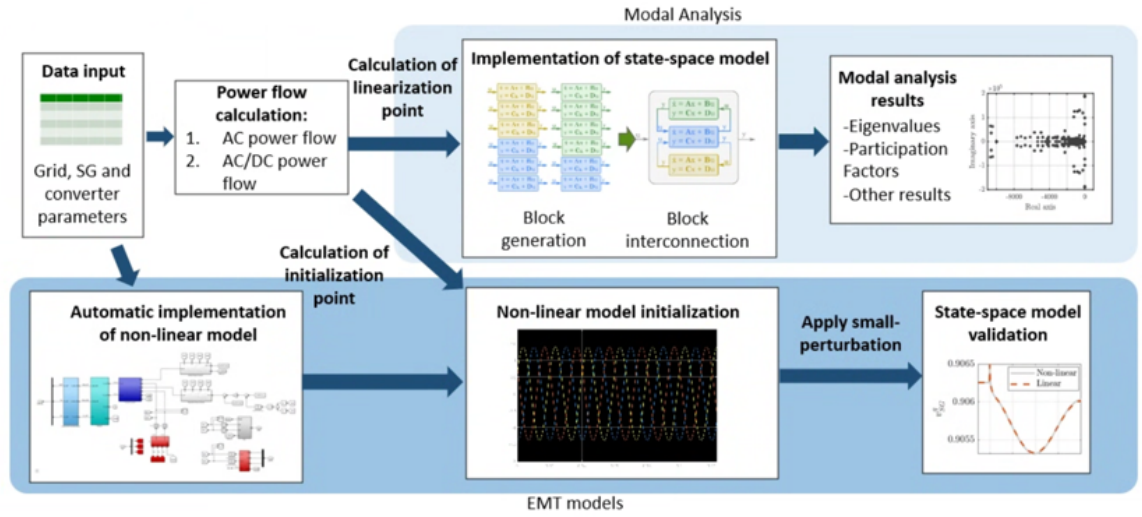

Figure 3: STAMP Tool Documentation Workflow.

Key features of STAMP include:

- Automated generation of state-space and nonlinear Simulink models,
- A predefined library of linear and nonlinear component models,
- Stability analysis across a wide frequency range, from inter-area to harmonic modes,
- High modularity and extensibility for custom applications.

1.3 Scope and Objectives

This report presents a comprehensive small-signal stability study of the Brazilian network under progressive replacement of synchronous generation by VSCs. The primary objectives and the workflow defined are to:

- **Stabilize the benchmark system** with the existing STAMP tool features;
- **Extract critical oscillatory modes** via eigenvalue, frequency and damping modal analysis;

- **Participation Factor Matrix Analysis** for better understanding of key interactions to tune;
- **Assess converter control impacts** by varying inner loop gains, and outer loop parameters;
- **Asses stability margin** and identify inter-area candidates.

The presented workflow was conducted on the base case, a VSC type Grid Following (GFOL) replacement, and a Second VSC GFOL addition.

2 The Brazilian 7-Bus Benchmark System

2.1 Overview of the System

As previously mentioned in chapter 1, the Brazilian 7-bus model is a reduced dynamic equivalent of part of the Brazilian transmission network. This model is widely used for academic and industrial non linear stability studies and provides a relevant testbed for analyzing interactions between conventional synchronous machines and power electronic converters. The system under investigation comprises only of Hydro-generation stations with two distinct areas based on the their voltage levels and primarily operating at 60 Hz frequency [4].

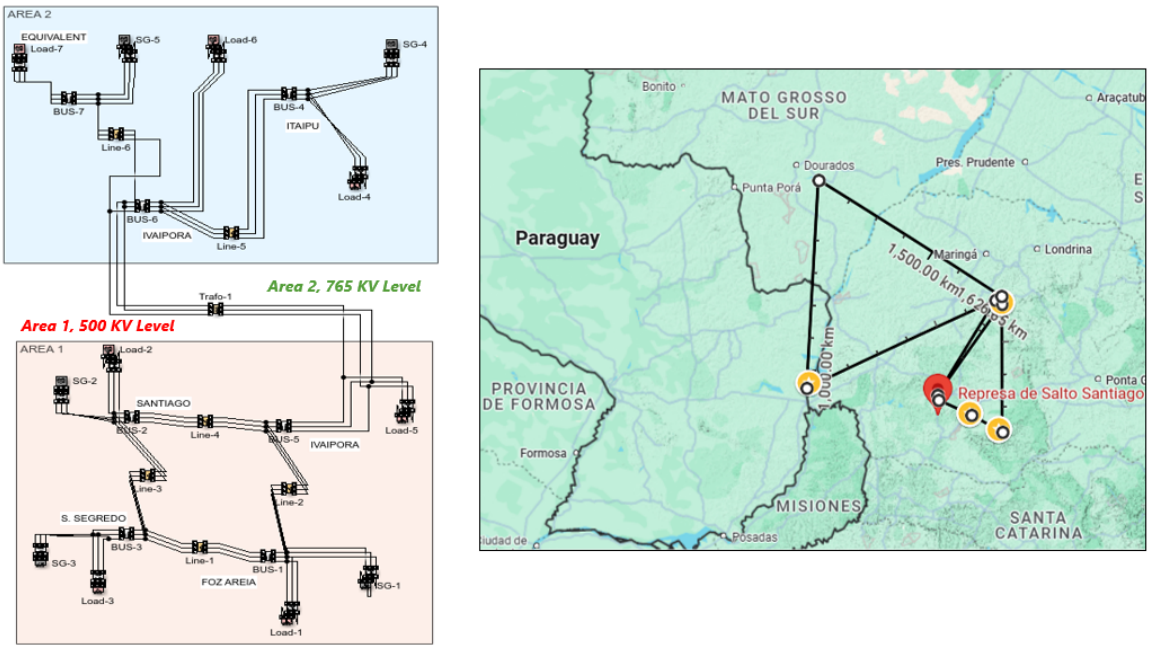

Figure 4: System's topology and power plant location.

The network consists of:

- 7 Buses,
- 5 Synchronous Generators,
- 1 Transformer connecting the two areas,
- AC transmission lines connecting the network.

2.2 Model and Network Parameter for the Power Flow

The single-line diagram's power flow results are displayed in the figure below, with all bus and load information listed in Tables 1 and 2. Table 3 contains the transmission line parameters, given in per-unit on a 1,000 MVA system base; each line is modeled as a series RL impedance, while the lines' capacitive charging has been converted into equivalent shunt reactors and

included in Table 4. Transformer parameters, also per-unit on the 1,000 MVA base, appear in Table 5, and generator data are summarized in Table 6. Each machine's maximum real power matches its MVA rating, and its reactive capability is set by a 0.8 power factor. Note that generator step-up transformers are omitted in this analysis.

Table 1: Bus Data and Power Flow Solution

Bus	Name	Base kV	Type	Voltage (pu)	Angle (°)
1	FOZ AREIA	500.0	PV	1.0300	24.53
2	S. SANTIAGO	500.0	PV	1.0300	27.22
3	S. SEGREDO	500.0	PV	1.0290	26.60
4	ITAIPU	765.0	PV	1.0390	48.45
5	IVAIPORA	500.0	PQ	0.9984	21.20
6	IVAIPORA	765.0	PQ	0.9895	21.45
7	EQUIVALENT	765.0	Swing	0.9660	0.00

Table 2: Load Data

Bus	P (MW)	Q (MVAr)
1	2405.0	–467.0
2	692.3	–184.0
3	688.2	–235.0
4	62.6	24.3
5	845.8	–9.2
6	–4.9	79.8
7	2884.0	–196.0

Table 3: Shunt Data

Bus	Name	Base kV	G_{shunt} (MW)	B_{shunt} (MVAr)
1	FOZ AREIA	500.0	0.0	179.2
2	S. SANTIAGO	500.0	0.0	149.1
3	S. SEGREDO	500.0	0.0	114.2
4	ITAIPU	765.0	0.0	36.8
5	IVAIPORA	500.0	0.0	33.0
6	IVAIPORA	765.0	0.0	2142.0
7	EQUIVALENT	765.0	0.0	42.0

Table 6: Power Flow Generator Data

Bus	V_{Sched} (pu)	P_{gen} (MW)	Q_{gen} (MVAr)	P_{max} (MW)	Q_{max} (MVAr)	Q_{min} (MVAr)	M_{base} (MVA)
1	1.030	1658.0	-412.3	1900	1140	-1140	1900
2	1.030	1332.0	-200.3	1400	840	-840	1400
3	1.029	1540.0	-446.7	1944	1166	-1166	1944
4	1.039	6500.0	1957.9	6633	3980	-3980	6633
7	0.966	-3164.3	952.3	3000	3600	-3600	6000

Table 4: Transmission Line Data (1,000 MVA Base)

From Bus	To Bus	R (pu)	X (pu)	B_c (pu)
1	3	0.0030	0.0380	0.0
1	5	0.0190	0.2450	0.0
2	3	0.0050	0.0760	0.0
2	5	0.0150	0.2250	0.0
4	6	0.0029	0.0734	0.0
6	7	0.0040	0.0570	0.0

Table 5: Transformer Data (1,000 MVA Base)

From Bus	To Bus	R (pu)	X (pu)	Tap (pu)
5	6	0.000	0.039	1.000

2.3 Dynamic Modeling and simulation

Dynamic simulation models and their parameters for the base-case were sourced from the PSS®E setup described in [4].

- **Generators**: Represented using `GENSAE` and `GENROU` models (salient-pole and round-rotor).
- **Exciters**: Modeled using `ST1` standard excitation systems.
- **PSS (Power System Stabilizers)**: Applied to all generators except the equivalent bus or interconection with the rest of the system (slack bus as well).
- **Loads**: Modeled as constant impedance.

This model in its original form does not include any HVDC link or Inverter Based Resources (IBR) and it has presented records of marginal stability, poor controllability and observability.

Table 7: Dynamic Model Data for Salient Pole Units (PSS®E Model GENSAE)

Description	Symbol	Unit	1 (FOZ AREIA)	2 (S. SANTIAGO)
Rated apparent power	MBASE	MVA	1900	1400
d-axis open-circuit transient time constant	T'_{do}	s	5.0	5.0
d-axis open-circuit sub-transient time constant	T''_{do}	s	0.053	0.053
q-axis open-circuit sub-transient time constant	T''_{qo}	s	0.123	0.123
Inertia	H	MW·s/MVA	4.5	4.5
Speed damping	D	pu	0.0	0.0
d-axis synchronous reactance	X_d	pu	0.85	0.85
q-axis synchronous reactance	X_q	pu	0.7	0.7
d-axis transient reactance	X'_d	pu	0.3	0.3
sub-transient reactance ($X''_d = X''_q$)	X''_d	pu	0.2	0.2
Leakage reactance	X_ℓ	pu	0.15	0.15
Saturation factor at 1.0 pu voltage	$S(1.0)$	—	0.001	0.001
Saturation factor at 1.2 pu voltage	$S(1.2)$	—	0.01	0.01
Rated field current	$I_{FDrated}$	pu	1.66	1.66

Table 8: Dynamic Model Data for Salient Pole Units (PSS®E Model GENSAE) (cont.)

Description	Symbol	Unit	3 (S. SEGREDO)	4 (ITAIPU)	7 (EQUIVALENT)
Rated apparent power	MBASE	MVA	1944	6633	6000
d-axis open-circuit transient time	T'_{do}	s	5.0	7.6	8.0
d-axis open-circuit sub-transient time	T''_{do}	s	0.06	0.09	0.09
q-axis open-circuit sub-transient time	T''_{qo}	s	0.09	0.19	0.20
Inertia	H	MW·s/MVA	4.5	5.07	5.0
Speed damping	D	pu	0.0	0.0	0.0
d-axis synchronous reactance	X_d	pu	0.88	0.90	1.00
q-axis synchronous reactance	X_q	pu	0.69	0.68	0.70
d-axis transient reactance	X'_d	pu	0.30	0.30	0.30
sub-transient reactance ($X''_d = X''_q$)	X''_d	pu	0.20	0.24	0.25
Leakage reactance	X_ℓ	pu	0.15	0.18	0.18
Saturation factor at 1.0 pu voltage	$S(1.0)$	—	0.001	0.001	0.001
Saturation factor at 1.2 pu voltage	$S(1.2)$	—	0.010	0.010	0.010
Rated field current	I_{FDrated}	pu	1.68	1.70	1.79

2.4 Excitation System Model and Parameters

Every generator uses the same excitation scheme, modeled here by the simplified ST1 exciter from PSS®E (see Fig.5). The model's parameter values are listed in Table below. The default model considers a simplified excitation system shown in the Fig. The choice of the upper and lower voltage limits ($E_{\max}$ and $E_{\min}$) to were considered to be very large so that they remain inactive and do not influence the small-signal stability outcomes.

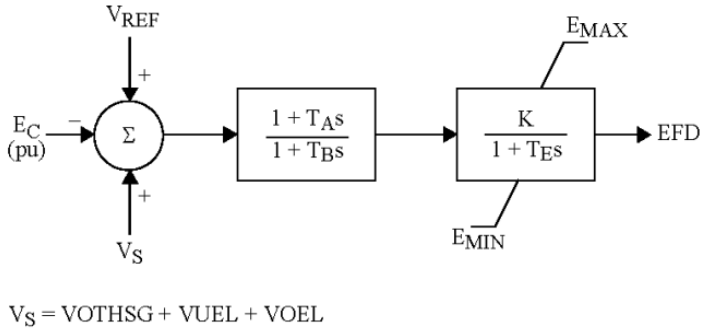

Figure 5: IEEE ST1 Simplified Block diagram

Table 9: Dynamic Model Data for the Simple Excitation System (PSS®E Model SEXS)

Description	**Symbol**	**Value**	**Unit**
TGR block 1 transient gain	T_A/T_B	1	—
TGR block 1 denominator time constant	T_B	1	s
Exciter gain	K	30	pu
Exciter time constant	T_E	0.05	s
Minimum AVR output	E_{min}	-4	pu
Maximum AVR output	E_{max}	5	pu

2.5 Power System Stabilizer Model and Parameters

The benchmark system installed Power Systems Stabilizers (PSS) at all generators except the equivalent unit at bus 7. Each PSS derives its input from rotor speed deviation and employs a common structure. The IEEE Std. 421.5-2005 specifies the PSS1A model was implemented by default, in this work we implement the PSS2A configuration. Fig. 7 shows the PSS2A block diagram, and Table 10 and Fig.6 lists the associated parameters.

A	B	C	D	E	F	G	H	I	J	K	L	M	N	O	P	Q	R	S
number	bus	Ks1	Ks2	Ks3	Tw1	Tw2	Tw3	Tw4	T1	T2	T3	T4	T6	T7	T8	T9	N	M
1	1	17.069	0.158	1	2	2	2	0	0.28	0.04	0.28	0.12	0	2	0	0.1	1	5
2	2	17.069	0.158	1	2	2	2	0	0.28	0.04	0.28	0.12	0	2	0	0.1	1	5
3	3	17.069	0.158	1	2	2	2	0	0.28	0.04	0.28	0.12	0	2	0	0.1	1	5
4	4	17.069	0.158	1	2	2	2	0	0.28	0.04	0.28	0.12	0	2	0	0.1	1	5
5	7	17.069	0.158	1	2	2	2	0	0.28	0.04	0.28	0.12	0	2	0	0.1	1	5

Figure 6: PSS2A Model parameters

Table 10: Dynamic Model Data for Power System Stabilizers (PSS®E Model IEEEST -PSS1A)

Description	**Symbol**	**Unit**	**Buses 1, 2, 3**	**Bus 4**
2nd order denominator coefficient	A_1	—	0	0
2nd order denominator coefficient	A_2	—	0	0
2nd order numerator coefficient	A_3	—	0	0
2nd order numerator coefficient	A_4	—	0	0
2nd order denominator coefficient	A_5	—	0	0
2nd order denominator coefficient	A_6	—	0	0
1st lead–lag numerator time constant	T_1	s	0.30	0.52
1st lead–lag denominator time constant	T_2	s	0.075	0.065
2nd lead–lag numerator time constant	T_3	s	0.30	0.52
2nd lead–lag denominator time constant	T_4	s	0.075	0.065
Washout block numerator time constant	T_5	s	3	3
Washout block denominator time constant	T_6	s	3	3
PSS gain	K_S	pu	10	16
PSS maximum output	$LS_{\max}$	pu	0.1	0.1
PSS minimum output	$LS_{\min}$	pu	-0.1	-0.1
Upper voltage limit for PSS operation	VC_U	pu	0	0
Lower voltage limit for PSS operation	VC_L	pu	0	0

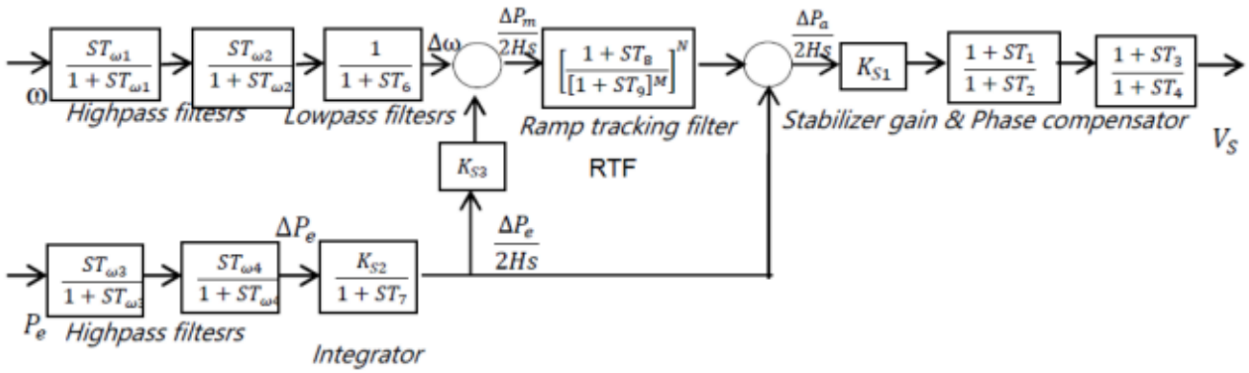

Figure 7: PSS 2A Block diagram.

2.6 Modeling Domains

The modeling is performed in two primary domains:

- **Small-signal (state-space) domain:** Used for linearization around a steady-state operating point. It facilitates modal analysis through eigenvalue computation, revealing system damping, frequency, and modal participation.
- **EMT domain:** A nonlinear time-domain model is built in Simulink for validation and transient simulation. This enables cross-verification of small-signal results and investigation of nonlinear phenomena such as saturation or controller limit activation.

2.7 Modeling Approach: STAMP Tool for Small-Signal and EMT Analysis

The modeling process using STAMP follows a structured pipeline:

2.8 Input Data Preparation

The power system components are defined using five Excel files:

1. `CASE.xlsx`: General topology, power flow configuration, simulation settings.
2. `CASE_data_sg.xlsx`: Synchronous generator parameters.
3. `CASE_data_vsc.xlsx`: VSC control and electrical parameters.
4. `CASE_data_shunt.xlsx`: Shunt and impedance data.
5. `CASE_data_ipc.xlsx`: Data for interconnecting power converters.

2.9 Power Flow and Initialization

The tool computes the power flow using either direct excel data or built-in solvers like MATPOWER. The steady state solution is used to initialize all nonlinear elements (voltage levels, currents, angles) required for model construction.
Results of converging power flow using the tool are shown below.

Bus	Voltage		Generation		Load	
#	Mag(pu)	Ang(deg)	P (MW)	Q (MVAr)	P (MW)	Q (MVAr)
1	1.028	24.497	1658.00	-412.30	2405.00	-646.20
2	1.028	27.201	1332.00	-200.30	692.30	-333.10
3	1.027	26.581	1540.00	-446.70	688.20	-349.20
4	1.041	48.301	6500.00	1957.90	62.60	-12.50
5	0.999	21.156	-	-	845.80	-42.20
6	0.991	21.402	-	-	-4.90	-2062.20
7	0.966	0.000*	-3165.16	916.98	2884.00	-238.00
		Total:	7864.84	1815.58	7573.00	-3683.40

Figure 8: Power Flow Results in STAMP Tool.

2.10 Linear Model Generation

From the steady state point, each component's state-space representation is constructed using built-in libraries. These include:

- Synchronous generators;
- Voltage source converters (VSC) GFOL, GFOR or STATCOM;
- Shunt elements (capacitors, reactors);
- Transformer and PI-line models.

These subsystems are then assembled into a global system model using the superposition property of linear systems[5].

2.11 Modal Analysis

Once the linear system is built, STAMP computes eigenvalues and participation factors to identify oscillation modes, their frequencies, damping ratios, and involved states. Additionally, study on the frequency domain interaction between SGs, VSCs and the grid can be performed. Modal (eigenvalue) analysis provides fundamental insight into a system's oscillatory behavior by examining the linearized state space model around an operating point. Each eigenvalue pair of the form:

$$\lambda = \sigma \pm j\omega \tag{1}$$

maps to a mode whose frequency:

$$f = \frac{\omega}{2\pi} \quad \text{(typically } < 1 \text{ Hz and } > 500 \text{ Hz)} \tag{2}$$

and damping ratio:

$$\zeta = \frac{-\sigma}{\sqrt{\sigma^2 + \omega^2}} \quad \text{(typically } < 10\% \text{ for critical modes)} \tag{3}$$

quantify its oscillation speed and decay rate.
In converter dominated scenarios, not only do classical electromechanical modes shift, but converter control loops (e.g., PLLs, inner current controllers, P–f droop) and network impedances interact to yield high frequency modes that can threaten stability if left unaddressed [6].

In conventional power systems, the rotational inertia of large SGs provides a natural damping against frequency deviations and underpins the classic small signal stability analysis in the phasor (RMS) domain. Oscillatory modes ranging from local intra-plant swings at 0.7–2 Hz to inter-area modes around 0.1–0.7 Hz—have long been well understood and mitigated via power system stabilizers (PSS), governor tuning, and network reinforcement [4]. However, as synchronous capacity is supplanted by VSCs, the grid's kinetic energy reserve dwindles and control induced resonances appear at higher frequencies (10 Hz–several kHz), including subsynchronous control interactions (SSCI) and harmonic instabilities [7].

2.11.1 Frequency categories

As mentioned previously, three main parameters were used to discriminate modes and identify critical candidates. Among all the poorly damped modes with $\zeta < 10\%$, low and high frequencies were prioritized, meaning by low frequencies those with $\omega < 1\,\text{Hz}$, which are typically associated with slow controllers and possible inter-area oscillations, and by high frequencies those with $\omega > 500\,\text{Hz}$, which are commonly linked to the switching dynamics of the converter. Nevertheless, the following table introduces the main categories of frequency ranges useful to identify possible causes of instability and their associated damping components.

Classification by Frequency Range and Mode Type

Oscillation Type	Frequency Range	Typical Cause	Involved Elements
Slow Control Modes	< 0.5 (can vary)	Governor Action, AVR	PSS, Generator excitation systems
Intra/Inter-Area Modes	0.5 – 2 Hz	Swinging of groups of generators with or across regions	Two or more generator in same area/ other areas
Torsional Modes	10 – 50 Hz	Shaft torsional resonance	Turbine–generator shaft system
Sub-Synchronous Oscillations (SSO)	10 – 60 Hz	SSR, SSCI, SSTI	Long lines, series compensation, converters
Harmonic Modes	≥ 100 Hz – several kHz	Resonance, converters, filters, PLL dynamics	Power electronics, filters, network RLC path

Figure 9: Classification of Frequency and Modes of Oscillations in Power Systems

2.12 Nonlinear Simulink Model Creation

STAMP generates a full EMT model using pre-configured Simulink blocks from the internal library (`myLibrary.slx`). This model reproduces the nonlinear dynamics of the network, including:

- Grid-following and grid-forming converter control
- Filter resonance
- Saturation and controller limits

It enables validation of modal results and analysis of fault conditions or controller responses.

3 Results and Discussion on Analysis Using STAMP Tool for Small-Signal and Modal Analysis

In the base-case scenario, five synchronous generators were modeled along with the other elements of the network. The system was observed to be unstable and stability efforts was applied towards tuning the system to obtain a stable system. The workflow is shown in the Fig.10 below.

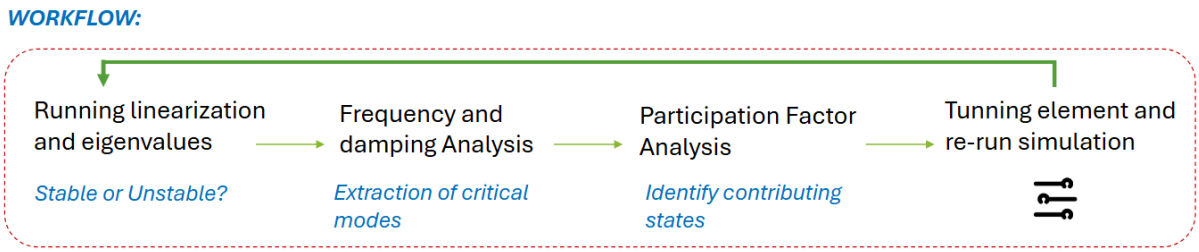

Figure 10: Workflow for performing analysis using STAMP Tool.

3.1 Case 1: Synchronous Generation (Base case) System

The base case unstable network provided a benchmark for analyzing the the different scenarios. In the modal table shown in Fig. 11a it can be easily seen that there is one unstable mode with all the eigenvalue on the right half plane, excluding the nominal frequencies. Based on this criteria, a conscience analysis of the data in the Fig.11a can be observed.

Mode	Real	Imaginary	Frequer	Dampin
1	0.195314522	0	0	-100%
13	-0.397541089	4.942051305	0.786552	8%
14	-0.397541089	-4.94205131	0.786552	8%
51	-7.662950493	376.824746	59.97352	2%
52	-7.662950493	-376.824746	59.97352	2%
61	-9.706702522	376.8215356	59.97301	3%
62	-9.706702522	-376.821536	59.97301	3%
74	-12.74209665	376.9725535	59.99705	3%
75	-12.74209665	-376.972554	59.99705	3%
77	-16.23913093	376.9048339	59.98627	4%
78	-16.23913093	-376.904834	59.98627	4%
87	-27.27893905	376.9890989	59.99968	7%
88	-27.27893905	-376.989099	59.99968	7%
98	-456.8432021	5420.476869	862.6957	8%
99	-456.8432021	-5420.47687	862.6957	8%
100	-456.9243339	4666.505901	742.6975	10%
101	-456.9243339	-4666.5059	742.6975	10%
110	-1135.986844	20559.44184	3272.137	6%
111	-1135.986844	-20559.4418	3272.137	6%
112	-1136.026849	19805.46538	3152.138	6%
113	-1136.026849	-19805.4654	3152.138	6%

(a) Poorly damped Modes

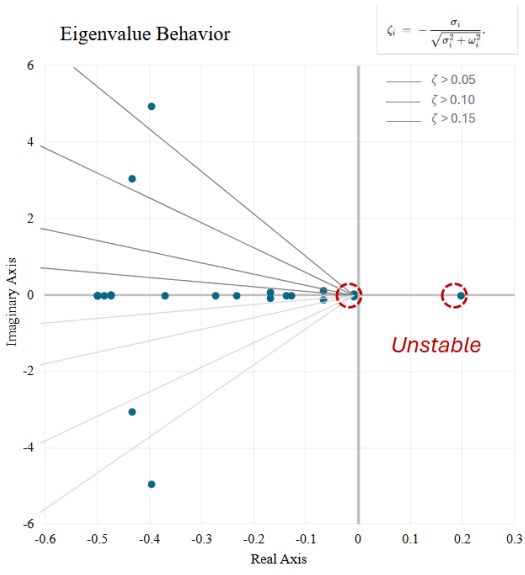

(b) Eigenvalue behavior

Figure 11: Base case dynamics.

From the above, the critical modes is shown in the Fig.12 below.

Extraction of critical modes table

Conjugate Pairs:	λ 1	λ 13-14	λ 98-99	λ 100-101	λ 110-111	λ 112-113
Real	0.1953	-0.3975	-456.8432	-456.9243	-1135.9868	-1136.0268
Imaginary	0	4.9421	5420.4769	4666.5059	20559.4418	19805.4654
Frequency	0	0.7866	862.6957	742.6975	3272.1368	3152.1377
Damping	-100%	8%	8%	10%	6%	6%

Figure 12: Critical modes as observed showing only low damped, low, and high frequency modes

3.1.1 Stabilization Effort of the Base case system

The stability effort to stabilize the system with only one eigenvalue on the right half plane was further carried out initially by tuning the parameters of the PSS of the Synchronous Generators, since this would have been thought of as the easier way of stabilizing the system. However, it was observed that the PSS gains and parameters had minimal effect on the system. As a result, the stabilization effort was channeled towards turning the gains of the Exciters of each generator until a range of stability was established. The Fig.17b shows the movement of the eigenvalue due to the tuning/ iteration of the exciter gain.

Further analysis of the base case scenario was performed taking a more closer look into the reduced participation factor matrix. Here the participation of each state corresponding to the element in the system was compared with their mode. The state impact on the mode was also classified with the a range of 0.3 and up to 1. The color scheme can also be used to easily visualize the different impact of the states on the modes. As seen in the figure, very thick dark shade represent the highest participation of 1 in any mode. While lighter shades to white indicate lesser to no impact of the state on the mode. A summary of the analysis is presented in the Fig.14 below.

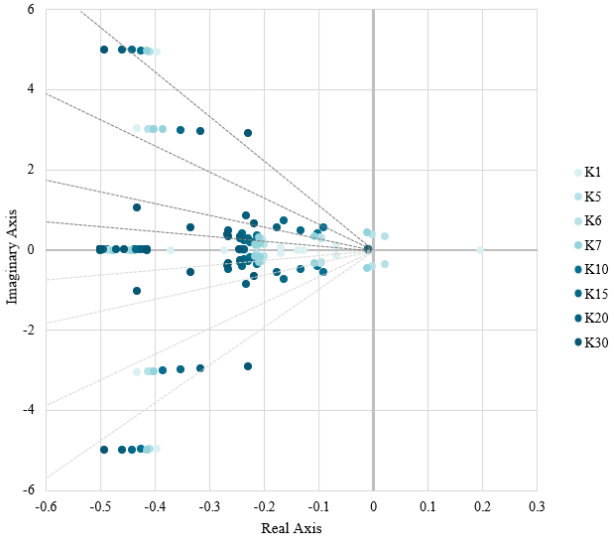

Figure 13: Exciter gain tuning.

Low damped, inter-area & high-frequency modes

Conjugate Pairs:	λ 1	λ 13-14	λ 98-99	λ 100-101	λ 110-111	λ 112-113
Real	0.1953	-0.3975	-456.8432	-456.9243	-1135.9868	-1136.0268
Imaginary	0.0000	4.9421	5420.4769	4666.5059	20559.4418	19805.4654
Frequency	0.0000	0.7866	862.6957	742.6975	3272.1368	3152.1377
Damping	-100%	8%	8%	10%	6%	6%
NET.iq13	0.00	0.00	0.79	0.79	0.00	0.00
NET.id13	0.00	0.00	0.79	0.79	0.00	0.00
NET.iq23	0.00	0.00	0.41	0.41	0.00	0.00
NET.id23	0.00	0.00	0.41	0.41	0.00	0.00
NET.iq46	0.00	0.01	0.00	0.00	0.41	0.41
NET.id46	0.00	0.00	0.00	0.00	0.41	0.41
Load3.voq	0.00	0.00	1.00	1.00	0.00	0.00
Load3.vod	0.00	0.00	1.00	1.00	0.00	0.00
Load4.voq	0.00	0.00	0.00	0.00	1.00	1.00
Load4.vod	0.00	0.00	0.00	0.00	1.00	1.00
States SG1.is_d	0.08	0.61	0.01	0.01	0.00	0.00
SG1.if_d	0.05	0.58	0.00	0.00	0.00	0.00
SG1.w_pu	0.00	0.63	0.00	0.00	0.00	0.00
SG1.e_th	0.00	0.90	0.00	0.00	0.00	0.00
SG2.is_d	0.02	0.37	0.01	0.01	0.00	0.00
SG2.if_d	0.01	0.34	0.00	0.00	0.00	0.00
SG2.w_pu	0.00	0.41	0.00	0.00	0.00	0.00
SG2.e_th	0.00	0.59	0.00	0.00	0.00	0.00
SG3.is_d	0.07	0.65	0.09	0.05	0.00	0.00
SG3.if_d	0.04	0.60	0.00	0.01	0.00	0.00
SG3.w_pu	0.00	0.71	0.00	0.00	0.00	0.00
SG3.e_th	0.00	1.00	0.00	0.00	0.00	0.00
SG4.is_q	0.00	0.00	0.00	0.00	0.43	0.40
SG4.is_d	1.00	0.16	0.00	0.00	0.44	0.39
SG4.if_d	0.70	0.14	0.00	0.00	0.01	0.01
SG4.e_th	0.01	0.72	0.00	0.00	0.00	0.00
SG5.is_d	0.65	0.03	0.00	0.00	0.00	0.00
SG5.if_d	0.45	0.03	0.00	0.00	0.00	0.00
Conjugate Pairs:	λ 1	λ 13-14	λ 98-99	λ 100-101	λ 110-111	λ 112-113
Interactions	SG4, SG5	SG1,2,3,4	Network 1-3, Load 3	Network 1-3, Load 3	SG4, Network 4-6, Load 4	SG4, Network 4-6, Load 4
Frequency Range	0 Hz (pure instability) Slow mode	Electromechanical	> 800 Hz Grid LC	> 700 Hz Grid LC	> 3000 Hz Grid LC	> 3000 Hz Grid LC
Damping component	Exciter / SG4 interaction failure	PSS SGs	Grid LC	Grid LC	Grid LC	Grid LC
Inter-area oscillation	No	Yes	No	No	No	No

Figure 14: Analysis of the Participation Factor Matrix for the Unstable base case

3.1.2 Inter-Area Oscillation candidate mode

In order to understand and validate the inter-area modes observed between the Synchronous Generators, it was important to take a deeper delve into the Right eigenvector analysis. The corresponding values were extracted as shown in the Fig.15 and a plot of the Generator swing was carried out in order to observe the directions of their vector. It can be clearly seen from the Fig that SG4 has a vector direction pointing in the opposite direction as the SGs. This confirms the existence of low damp, low frequency inter-area oscillations in the base case system among the SGs.

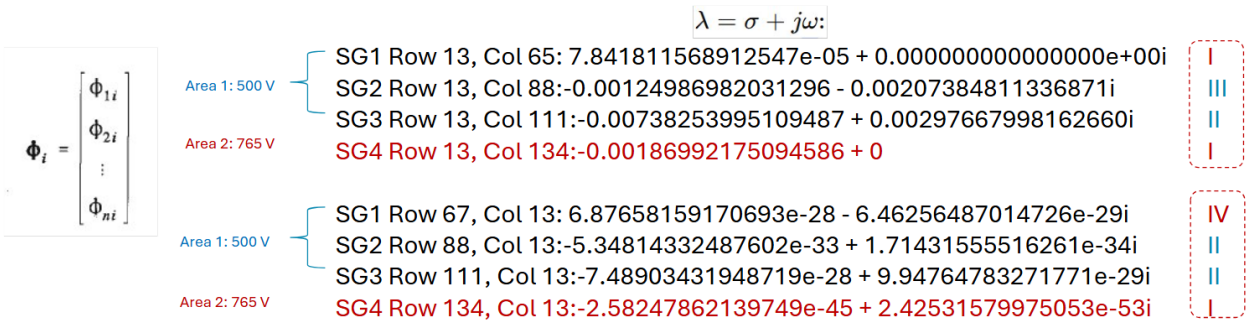

Figure 15: Right Eigen Vector Analysis

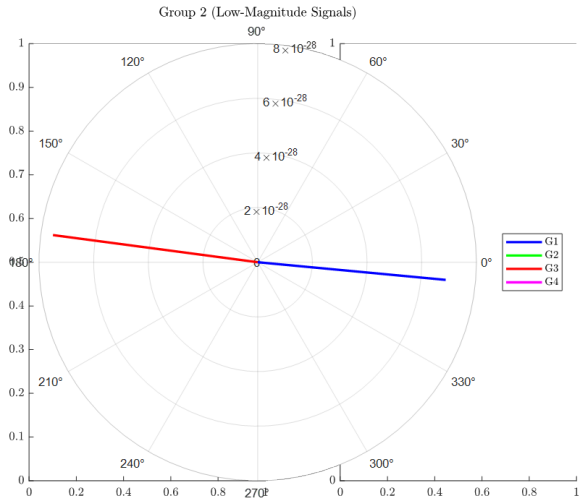

Figure 16: SG4 Swing against SGs 1 with plot of the Right Eigen Vectors

3.1.3 Base Case – Stabilization Results

From the analysis and iterations of the exciter gains, the most stable gain was obtained at K = 30. At this gain value, the system exhibit minimal and reduced dynamics and the eigenvalue was observed to be further away from the origin and right half plane, this is shown in the Fig.17a below.

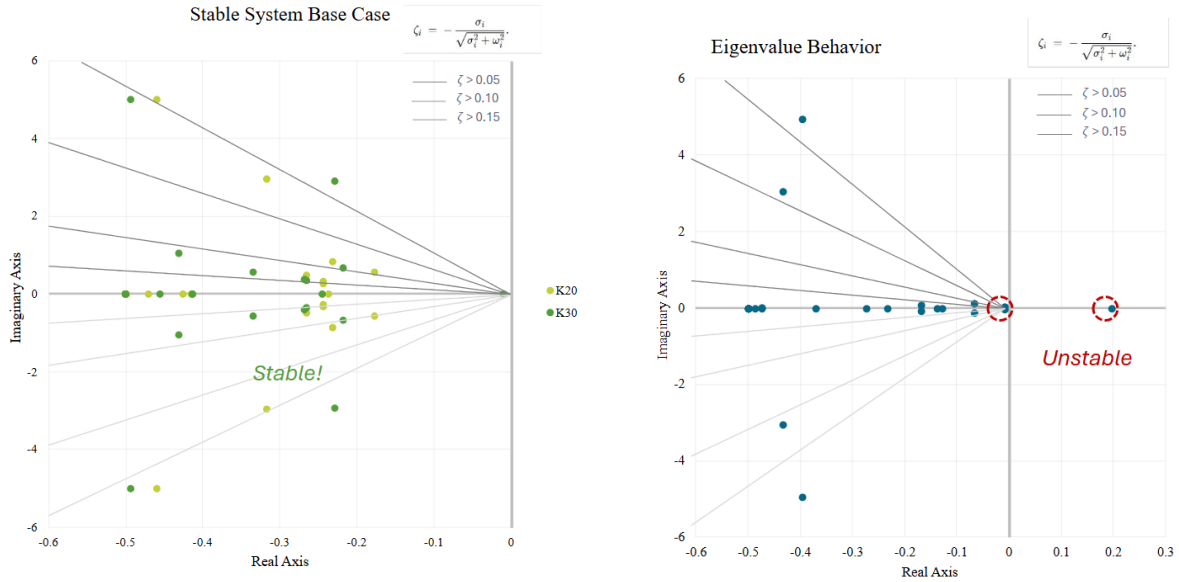

(a) Stable System

(b) Initial Unstable System

Figure 17: Base case stabilization.

The participation factor matrix was also analyzed with insights and observation presented on the table in the Fig.18 below.

Low damped, inter-area & high-frequency modes

Conjugate Pairs:	λ 1	λ 13-14	λ 98-99	λ 100-101	λ 110-111	λ 112-113
Real	-0.22947	-0.49326	-456.882	-456.934	-1135.98	-1136.02
Imaginary	2.920307	4.99891	5420.463	4666.496	20559.45	19805.5
Frequency	0.464781	0.7956	862.6934	742.696	3272.137	3152.14
Damping	8%	10%	8%	10%	6%	6%

NET.iq23	0.00	0.00	0.70	0.70	0.00	0.00
NET.id23	0.00	0.00	0.70	0.70	0.00	0.00
NET.iq25	0.00	0.00	0.23	0.23	0.00	0.13
NET.id25	0.00	0.00	0.23	0.23	0.00	0.13
NET.iq67	0.00	0.00	0.00	0.00	1.00	0.00
NET.id67	0.00	0.00	0.00	0.00	1.00	0.00
Trafo1.iq	0.00	0.00	0.01	0.01	0.00	0.76
Trafo1.id	0.00	0.00	0.01	0.01	0.00	0.76
Load1.vcq	0.00	0.00	0.41	0.41	0.00	0.00
Load1.vcd	0.00	0.00	0.41	0.41	0.00	0.00
Load2.vcq	0.00	0.00	1.00	1.00	0.00	0.00
Load2.vcd	0.00	0.00	1.00	1.00	0.00	0.00
Load5.vcq	0.00	0.00	0.00	0.00	0.00	1.00
Load5.vcd	0.00	0.00	0.00	0.00	0.00	1.00
Load6.vcq	0.00	0.00	0.00	0.00	0.14	0.01
Load6.vcd	0.00	0.00	0.00	0.00	0.14	0.01
Load7.vcq	0.00	0.00	0.00	0.00	0.86	0.00
Load7.vcd	0.00	0.00	0.00	0.00	0.86	0.00
SG2.pss1_1	0.00	0.78	0.00	0.00	0.00	0.00
SG2.pss1_2	0.00	0.78	0.00	0.00	0.00	0.00
SG2.pss2_1	0.00	0.57	0.00	0.00	0.00	0.00
SG2.pss2_2	0.00	0.57	0.00	0.00	0.00	0.00
SG3.pss1_1	0.00	1.00	0.00	0.00	0.00	0.00
SG3.pss1_2	0.00	1.00	0.00	0.00	0.00	0.00
SG3.pss2_1	0.00	0.32	0.00	0.00	0.00	0.00
SG3.pss2_2	0.00	0.32	0.00	0.00	0.00	0.00
SG4.ig_x	0.81	0.00	0.00	0.00	0.00	0.00
SG4.ig_x	1.00	0.00	0.00	0.00	0.00	0.00

Conjugate Pairs:	λ 4-5	λ 18-19	λ 98-99	λ 100-101	λ 110-111	λ 112-113
Interactions	SG4	All PSS in Area 1	Load 1-2, Network	Load 1-2, Network	Load 6-7, Network Slack	V Load 5, Transformer
Frequency Range	Slow Controller	Electromechanical Rotor	High Frequency (Cables)	High Frequency (Cables)	Very High Frequency (Cables)	Very High Frequency (Cables)
Damping component	Governor Action	PSS	Grid LC (passive)	Grid LC (passive)	Grid LC (passive)	Grid LC (passive)
Inter-area oscillation	No	No	No	No	No	No

Figure 18: Participation Matrix Analysis of Stable Base case system

3.2 Synchronous Generator Replacement with a Voltage Source Converter - Grid Following (VSC - GFOL)

The next scenario involves gradual replacement of the Synchronous Generators (SGs) with a Voltage Source Converter. The aim of this analysis is to study the small signal stability and dynamics the high inertia based system responds to the integration of IBRs with lower inertia capacities. The implementation follows a similar approach, first, the parameters of the VSC was modeled on the excel sheet and the STAMP Tool based on the standardized GFOL. One of the Synchronous Generator on bus 4 was completely taken out and replaced with an equivalent sized VSC, this was done in order to maintain the convergence of the power flow results and also establish a basis for the dynamic simulation since the system is highly non linear, a small variation of the model parameters are likely to cause a larger deviation in the results obtained. The Non linear model of the new case is shown in the Fig.19 and the model parameters of the VSC is also shown in the table presented in Fig.20

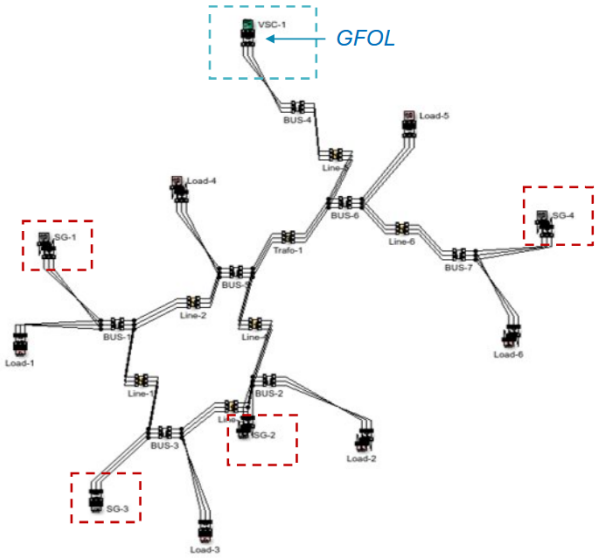

Figure 19: Non-Linear Model Topology of Network with one SG replaced by VSC at bus 4

A	B	C	D	E	F	G	H	I	J	K	L	M	N	O	P	Q	R	S	T
number	bus	Rtr	Xtr	Rc	Xc	Bac	Rac	tau_s	ts_pll	xi_pll	tau_p	tau_q	:au_droop_	k_droop_f	:au_droop_u	k_droop_u	tau_md	tau_cmd	tau_zoh
1	2	0.002	0.1	0.005	0.15	0.15	0.0001	0.001	0.707	0.1	1.1	1.1	0.1	0.5	0.5	2	-1	-1	-1

Figure 20: Parameters of the VSC Implemented in excel sheet of STAMP Tool

3.2.1 Analysis on Replacement of one Synchronous Generator with one VSC - GFOL - Unstable case

After swapping one synchronous generator for a grid-following VSC, the system went unstable with six eigenvalues moving into the right half-plane. Examining Fig.21 and Fig.22, it can be seen that the poorly damped, higher frequency modes originated from the VSC's filters and switching dynamics, while the low frequency, low damped oscillations arise from the remaining SGs' electromechanical interactions. This confirms that adding a VSC without extra damping can excite both fast converter related resonances and slower generator machine swings. A more closer look at the dynamics of the can be seen on the Participation Factor Matrix and Modal analysis in the table of Fig.22

State M	Real	Imaginar	Freque	Dampi	Freque
1	1776.07072	3210.361	510.945	-48%	425.631
2	1776.07072	-3210.361	510.945	-48%	425.631
3	1142.30355	7606.1668	1210.56	-15%	1196.83
4	1142.30355	-7606.167	1210.56	-15%	1196.83
5	52.30648	3166.6716	503.991	-2%	503.923
6	52.30648	-3166.672	503.991	-2%	503.923
10	-0.24937	2.83391	0.45103	9%	0.44928
11	-0.24937	-2.83391	0.45103	9%	0.44928
27	-0.54267	5.39463	0.85858	10%	0.85423
28	-0.54267	-5.39463	0.85858	10%	0.85423
49	-8.09193	376.81791	59.9724	2%	59.9586
50	-8.09193	-376.8179	59.9724	2%	59.9586
59	-12.74053	376.9715	59.9969	3%	59.9626
60	-12.74053	-376.9715	59.9969	3%	59.9626
68	-15.98885	376.89233	59.9843	4%	59.9303
69	-15.98885	-376.8923	59.9843	4%	59.9303
78	-27.27014	376.98834	59.9996	7%	59.8424
79	-27.27014	-376.9883	59.9996	7%	59.8424
88	-421.97853	4678.2539	744.567	9%	741.532
89	-421.97853	-4678.254	744.567	9%	741.532
90	-430.49772	5432.2956	864.577	8%	861.858
91	-430.49772	-5432.296	864.577	8%	861.858
100	-1135.98449	20559.446	3272.14	6%	3267.14
101	-1135.98449	-20559.45	3272.14	6%	3267.14
102	-1136.02485	19805.46	3152.14	6%	3146.95
103	-1136.02485	-19805.46	3152.14	6%	3146.95

(a) Poorly damped Modes

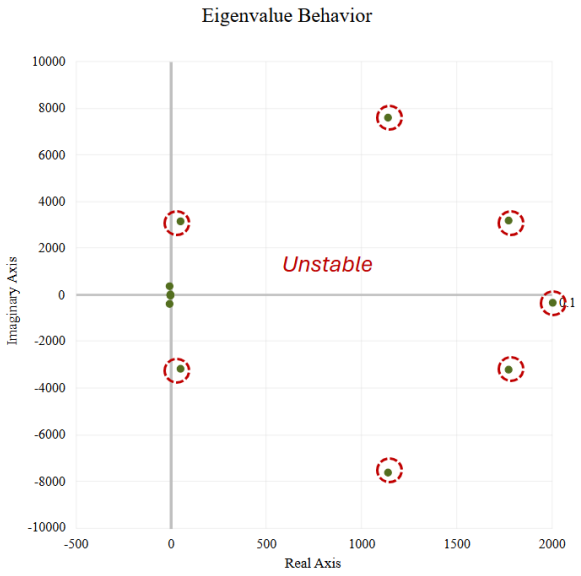

(b) Eigenvalue behavior

Figure 21: Case 1 dynamics.

Low damped, low and high-frequency modes

Conjugate Pairs:	λ 1-2	λ 3-4	λ 5-6	λ 10-11	λ 88-89	λ 90-91	λ 100-101	λ 102-103
Real	1776.071	1142.304	52.30648	-0.24937	-421.979	-430.498	-1135.98	-1136.02
Imaginary	3210.361	7606.167	3166.672	2.83391	4678.254	5432.296	20559.45	19805.46
Frequency	510.9448	1210.559	503.9914	0.45103	744.5672	864.5767	3272.137	3152.137
Damping	-48%	-15%	-2%	9%	9%	8%	6%	6%
States								
NET.iq13	0.02	0.00	0.24	0.00	0.73	0.78	0.00	0.00
NET.id13	0.00	0.00	0.02	0.00	0.79	0.74	0.00	0.00
NET.iq23	0.12	0.00	0.47	0.00	0.43	0.44	0.00	0.00
NET.id23	0.03	0.01	0.14	0.00	0.41	0.39	0.00	0.00
NET.iq46	0.00	0.00	0.00	0.01	0.00	0.00	0.41	0.41
NET.id46	0.00	0.00	0.00	0.00	0.00	0.00	0.41	0.41
Load2.vcq	0.35	0.03	1.00	0.00	0.18	0.18	0.00	0.00
Load3.vcq	0.02	0.00	0.11	0.00	0.95	1.00	0.00	0.00
Load3.vcd	0.01	0.00	0.03	0.00	1.00	0.95	0.00	0.00
Load4.vcq	0.00	0.00	0.00	0.00	0.00	0.00	1.00	1.00
Load4.vcd	0.00	0.00	0.00	0.00	0.00	0.00	1.00	1.00
SG3.is_q	0.00	0.00	0.00	0.00	0.00	0.00	0.43	0.40
SG3.is_d	0.00	0.00	0.00	1.00	0.00	0.00	0.44	0.39
SG3.if_d	0.00	0.00	0.00	0.96	0.00	0.00	0.01	0.01
SG3.w_pu	0.00	0.00	0.00	0.39	0.00	0.00	0.00	0.00
SG3.e_th	0.00	0.00	0.00	0.46	0.00	0.00	0.00	0.00
SG4.is_d	0.00	0.00	0.00	0.75	0.00	0.00	0.00	0.00
SG4.if_d	0.00	0.00	0.00	0.73	0.00	0.00	0.00	0.00
GFOL1.ig_q	1.00	0.19	0.66	0.00	0.07	0.05	0.00	0.00
GFOL1.ig_d	0.30	0.58	0.21	0.00	0.02	0.01	0.00	0.00
GFOL1.is_q	0.48	0.18	0.22	0.00	0.03	0.00	0.00	0.00
GFOL1.is_d	0.13	0.66	0.12	0.00	0.00	0.03	0.00	0.00
GFOL1.ucap_q	0.35	0.31	0.15	0.00	0.01	0.01	0.00	0.00
GFOL1.ucap_d	0.11	1.00	0.05	0.00	0.01	0.01	0.00	0.00
Interactions	GFOL, Load 2	GFOL cap	GFOL, AC Net, Load 2,	SG3, SG4	AC Net, Load	AC Net, Load	SG3, AC Net, Load	SG3, AC Net, Load
Frequency Range	Mid-High Freq. (VSC)	High (VSC)	Mid-High	Low	Mid-High	Mid-High	High	High
Damping component	Inner or outer controller	Filter	Filter	Gov. action	Cable/Line	Cable/Line	Electroma g., Gov. action	Electroma g., Gov. action
Inter-area oscillation	No	No	No	No	No	No	No	No

Figure 22: Participation Factor Matrix and Analysis after adding one VSC (Unstable case)

3.2.2 Stabilization of the network with one VSC - GFOL

Initially, An increase in the current controller gains to attenuate the new oscillations was made, but negligible improvement was observed in the overall system dynamics. Then attention was turned towards the outer power loop and modification of its time constant τ_{pq}. By varying τ_{pq}, the loop response was sufficiently slowed to introduce additional damping without compromising performance. This straightforward adjustment stabilized all previously unstable modes in few iterations and it proved to be more effective and simpler to tune than aggressive inner loop modifications.

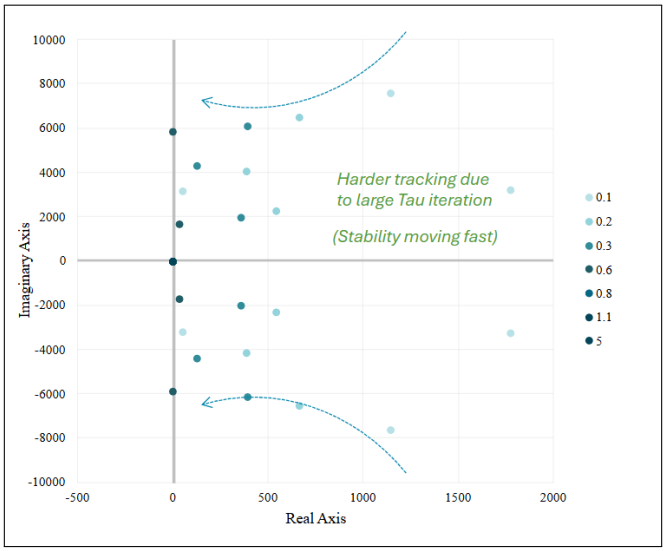

Figure 23: Eigenvalue plot showing the tuning of τ_{pq} after adding one VSC

Conjugate Pairs:	λ 1-2	λ 22-23	λ 81-82	λ 83-84	λ 88-89	λ 90-91	λ 100-101	λ 102-103
Real	-0.17537	-0.54062	-150.062	-181.943	-267.304	-305.591	-1135.98	-1136.02
Imaginary	2.767	5.39446	5789.089	4392.482	4823.042	5288.844	20559.45	19805.46
Frequency	0.44038	0.85856	921.3621	699.0853	767.611	841.7457	3272.137	3152.137
Damping	6%	10%	3%	4%	6%	6%	6%	6%
States								
NET.iq13	0.00	0.00	0.16	0.13	0.07	1.00	0.00	0.00
NET.id13	0.00	0.00	0.07	0.14	0.37	0.69	0.00	0.00
NET.iq23	0.00	0.00	0.47	0.21	0.26	0.14	0.00	0.00
NET.iq25	0.00	0.00	0.51	0.02	0.03	0.02	0.00	0.00
NET.iq46	0.00	0.01	0.18	0.00	0.00	0.00	0.41	0.41
NET.id46	0.00	0.00	0.18	0.00	0.00	0.00	0.41	0.41
Load1.vcq	0.00	0.00	0.21	0.03	0.01	0.33	0.00	0.00
Load1.vcd	0.00	0.00	0.35	0.03	0.10	0.21	0.00	0.00
Load2.vcq	0.00	0.00	0.32	0.36	0.55	0.25	0.00	0.00
Load2.vcd	0.00	0.00	0.09	0.49	0.24	0.08	0.00	0.00
Load3.vcq	0.00	0.00	0.05	0.21	0.17	0.98	0.00	0.00
Load3.vcd	0.00	0.00	0.12	0.24	0.47	0.76	0.00	0.00
Load4.vcq	0.00	0.00	0.00	0.00	0.00	0.00	1.00	1.00
Load4.vcd	0.00	0.00	0.00	0.00	0.00	0.00	1.00	1.00
Load6.vcq	0.00	0.00	1.00	0.00	0.00	0.00	0.00	0.00
Load6.vcd	0.00	0.00	1.00	0.00	0.00	0.00	0.00	0.00
SG1.is_d	0.23	0.67	0.03	0.00	0.00	0.01	0.00	0.00
SG1.if_d	0.30	0.62	0.01	0.00	0.00	0.00	0.00	0.00
SG1.w_pu	0.07	0.69	0.00	0.00	0.00	0.00	0.00	0.00
SG1.e_th	0.02	0.90	0.00	0.00	0.00	0.00	0.00	0.00
SG2.is_d	0.23	0.73	0.01	0.02	0.01	0.06	0.00	0.00
SG2.if_d	0.30	0.65	0.00	0.00	0.00	0.01	0.00	0.00
SG2.w_pu	0.07	0.78	0.00	0.00	0.00	0.00	0.00	0.00
SG2.e_th	0.02	1.00	0.00	0.00	0.00	0.00	0.00	0.00
SG3.exc_x1	0.34	0.00	0.00	0.00	0.00	0.00	0.00	0.00
SG3.pss1_x1	0.77	0.00	0.00	0.00	0.00	0.00	0.00	0.00
SG3.pss1_x2	0.31	0.00	0.00	0.00	0.00	0.00	0.00	0.00
SG3.is_q	0.00	0.00	0.13	0.00	0.00	0.00	0.43	0.40
SG3.is_d	1.00	0.18	0.14	0.00	0.00	0.00	0.44	0.39
SG3.if_d	0.60	0.16	0.02	0.00	0.00	0.00	0.01	0.01
SG3.e_th	0.08	0.41	0.00	0.00	0.00	0.00	0.00	0.00
SG4.is_d	0.33	0.07	0.24	0.00	0.00	0.00	0.00	0.00
SG4.if_d	0.40	0.07	0.05	0.00	0.00	0.00	0.00	0.00
GFOL1.ig_q	0.00	0.00	0.56	0.65	1.00	0.92	0.00	0.00
GFOL1.ig_d	0.00	0.00	0.16	1.00	0.34	0.49	0.00	0.00
GFOL1.is_q	0.00	0.00	0.89	0.03	0.12	0.18	0.00	0.00
GFOL1.ucap_q	0.00	0.00	0.32	0.41	0.54	0.56	0.00	0.00
GFOL1.ucap_d	0.00	0.00	0.09	0.74	0.18	0.41	0.00	0.00
Interactions	GFOL	GFOL	GFOL	SG2, Load 6	Network	Load 3	Load 4	Load 4
Frequency Range	Mid-High (VSC)	High (VSC)	High (VSC)	Low	High	High	High	High
Damping component	Inner or outer controller	Inner or outer controller	Inner or outer controller	Governor action	Cable/Line	Cable/Line	Electromagnetic + Gov. action	Electromagnetic + Gov. action
Inter-area oscillation	No	No	No	No	No	No	No	No

Figure 24: Participation Matrix Analysis after adding one VSC (Stable case)

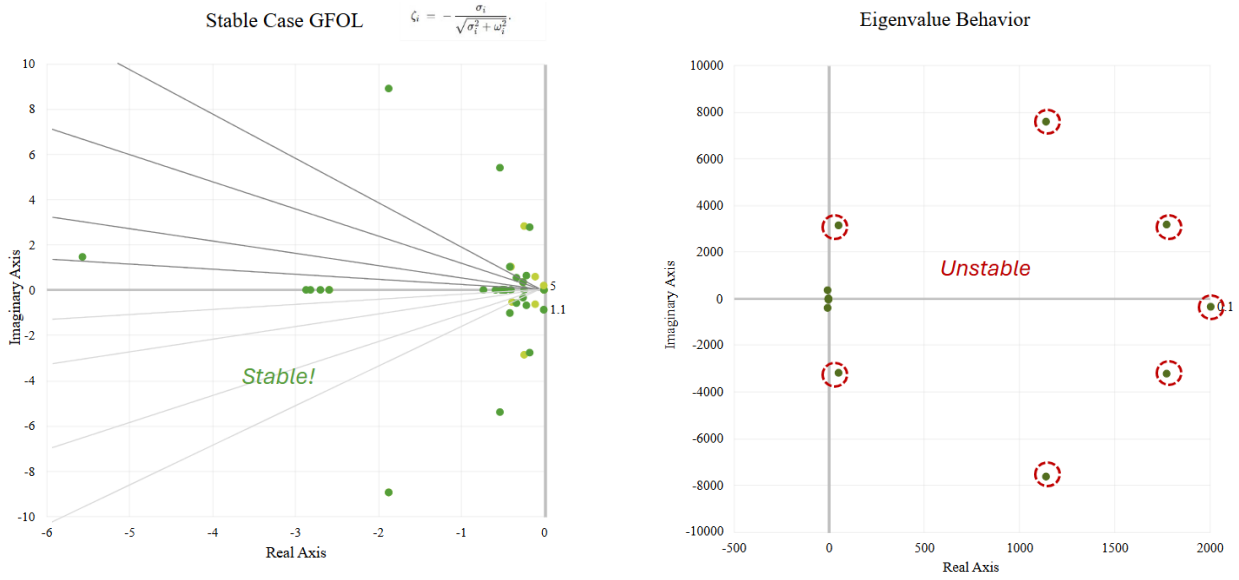

(a) Poorly damped Modes

(b) Eigenvalue behavior

Figure 25: Case 1 stabilization results.

The plot on Fig.25 shows the stabilized network with the VSC added and the participation of each states on the modes have been successfully analyzed.

3.3 Analysis on Replacement of 2 SGs with 2 VSCs - GFOL

We then removed two synchronous generators and replaced them with grid following VSCs. Almost immediately, overall inertia dropped significantly and several previously well damped electromechanical modes became lightly damped and even unstable. The two VSCs' current- and power loop control introduced new high frequency resonances from their filters and switching behavior, while the remaining generators experienced larger low frequency power swings. We relied on the tuning method applied in the previous scenario by tuning power loop time constant τ_{pq}, this yielded a stable system with all the eigenvalues on the left half plane. Tuning τ_{pq} between 1.0 and 1.18 resulted in a stable system. The interaction between states and mode can be seen in the Fig.27 below.

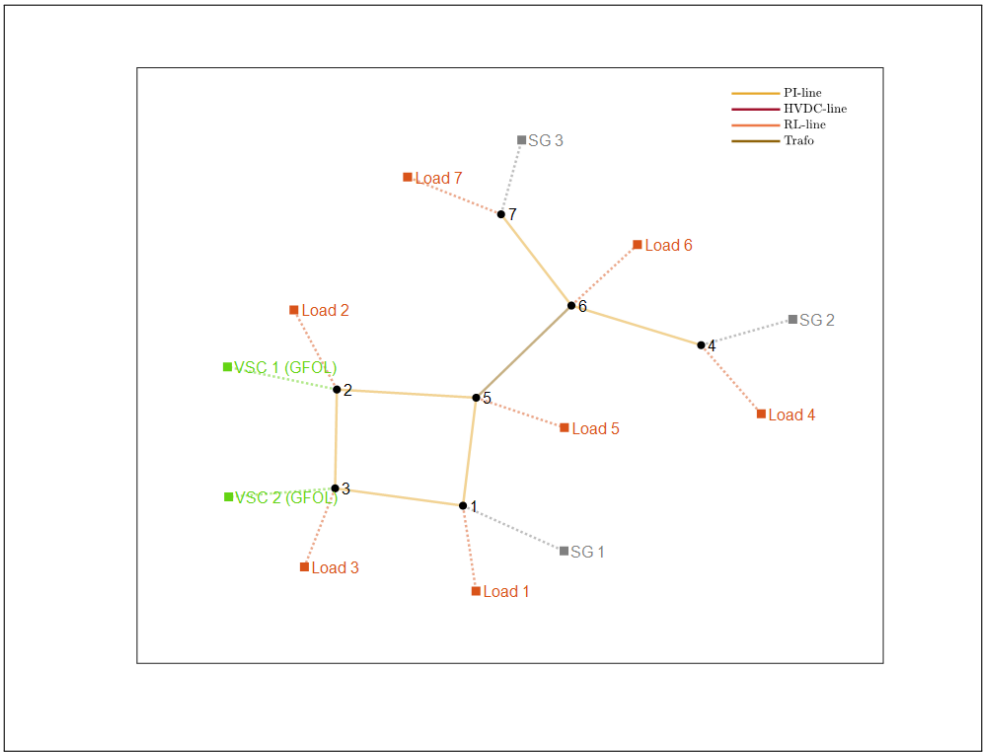

Figure 26: Network topology with integration of 2 VSC - GFOL

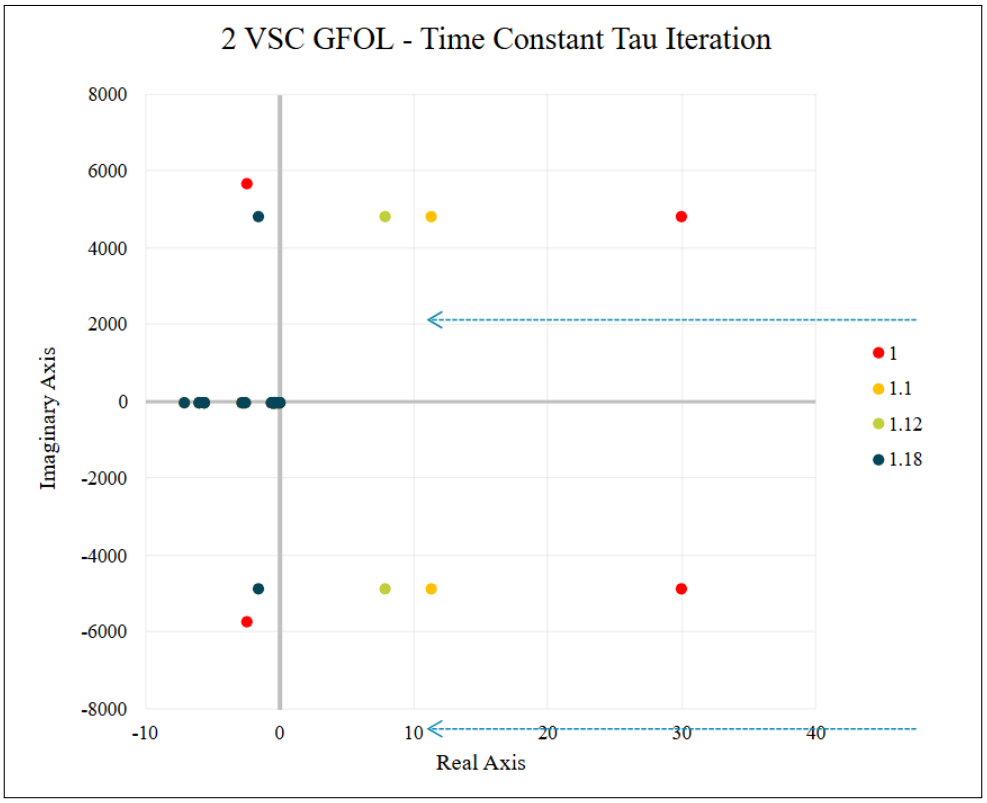

Figure 27: Eigenvalue movements of tuning unstable system with 2 VSC - GFOL from $\tau_{pq} = 1.1$ to 1.18

The unstable case of the system with 2 VSC - GFOL is shown in Fig.28 It can be observed that the interactions were mainly between the VSCs and other elements in the network. This high frequencies were mainly due to the converter switching dynamics. The presence of an inter-area oscillation can also be seen between SG2 and SG3. This low frequency, low damped inter-area oscillation have potentials of causing instability in the system especially with high penetration of IBR where the inertia is relatively lower.

Conjugate Pairs:	λ 1-2	λ 6-7	λ 55-56	λ 70-71	λ 74-75	λ 79-80	λ 83-84	λ 94-95	λ 96-97
Real	11.19	-0.17	-21.37	-115.77	-180.98	-225.72	-236.00	-1135.98	-1136.02
Imaginary	4846.07	2.67	5698.78	3201.01	4077.65	5780.39	6547.93	20559.45	19805.46
Frequency	771.28	0.42	906.99	509.46	648.98	919.98	1042.14	3272.14	3152.14
Damping	0%	6%	0%	4%	4%	4%	4%	6%	6%
NET.iq13	0.02	0.00	0.01	0.95	0.47	0.44	0.36	0.00	0.00
NET.id13	0.01	0.00	0.02	0.41	0.93	0.30	0.42	0.00	0.00
NET.iq46	0.00	0.01	0.00	0.00	0.00	0.00	0.00	0.41	0.41
NET.id46	0.00	0.00	0.00	0.00	0.00	0.00	0.00	0.41	0.41
Load1.vcq	0.01	0.00	0.00	0.64	0.27	0.08	0.06	0.00	0.00
Load1.vcd	0.00	0.00	0.00	0.21	0.48	0.05	0.07	0.00	0.00
Load2.vcq	0.41	0.00	0.22	0.04	0.02	0.11	0.09	0.00	0.00
Load2.vcd	0.20	0.00	0.33	0.01	0.05	0.08	0.11	0.00	0.00
Load3.vcq	0.03	0.00	0.02	0.29	0.16	1.00	0.84	0.00	0.00
Load3.vcd	0.01	0.00	0.03	0.15	0.41	0.72	1.00	0.00	0.00
Load4.vcq	0.00	0.00	0.00	0.00	0.00	0.00	0.00	1.00	1.00
Load4.vcd	0.00	0.00	0.00	0.00	0.00	0.00	0.00	1.00	1.00
SG2.is_q	0.00	0.00	0.00	0.00	0.00	0.00	0.00	0.43	0.40
SG2.is_d	0.00	1.00	0.00	0.00	0.00	0.00	0.00	0.44	0.39
SG2.if_d	0.00	0.97	0.00	0.00	0.00	0.00	0.00	0.01	0.01
SG2.w_pu	0.00	0.34	0.00	0.00	0.00	0.00	0.00	0.00	0.00
SG2.e_th	0.00	0.39	0.00	0.00	0.00	0.00	0.00	0.00	0.00
SG3.is_d	0.00	0.79	0.00	0.00	0.00	0.00	0.00	0.00	0.00
SG3.if_d	0.00	0.76	0.00	0.00	0.00	0.00	0.00	0.00	0.00
GFOL1.ig_q	1.00	0.00	0.62	0.09	0.03	0.07	0.06	0.00	0.00
GFOL1.ig_d	0.55	0.00	1.00	0.03	0.05	0.06	0.08	0.00	0.00
GFOL1.ucap_q	0.62	0.00	0.44	0.10	0.05	0.03	0.03	0.00	0.00
GFOL1.ucap_d	0.41	0.00	0.79	0.03	0.09	0.03	0.05	0.00	0.00
GFOL2.ig_q	0.10	0.00	0.06	0.90	0.41	0.86	0.78	0.00	0.00
GFOL2.ig_d	0.06	0.00	0.10	0.34	0.55	0.73	0.99	0.00	0.00
GFOL2.is_q	0.01	0.00	0.00	0.39	0.06	0.07	0.02	0.00	0.00
GFOL2.ucap_q	0.06	0.00	0.04	1.00	0.56	0.41	0.39	0.00	0.00
GFOL2.ucap_d	0.04	0.00	0.08	0.49	1.00	0.42	0.56	0.00	0.00
	1	6	55	70	74	79	83	94	96
				Eigenvalues					
Interactions	GFOL 1 ucap, ig qd & Load 2 vcq	SG2 is/fd, w, e & SG3 is/fd	GFOL 1 ucap, ig qd, & Load 2 vcd	GFOL 2, AC Net 13 & Load 1vcq	GFOL 2, AC Net 13, Load 1 & 3	Load 3 q voltages & GFOL 2 q currents	Load 3 d voltages & GFOL 2 d currents	Load 4 qd voltages & Network 4-6, SG2	Load 4 qd voltages & Network 4-6, SG2
Frequency Range	High (VSC)	Low	High (VSC)	High (VSC)	High (VSC)	High (VSC)	Very High (VSC)	Very High	Very High
Damping component	Filter	PSS, AVR, Gov. Action	Inner/outer loop & Filters	Inner/outer loop & Filters	Inner/outer loop & Filters	Inner/outer loop & Filters	Inner/outer loop & Filters	Cable/lines filters	Cable/lines filters
Inter-area oscillation	No	Yes	No	No	No	No	No	No	No

Figure 28: Reduced Participation Factor Matrix and Modal analysis for unstable mode with 2 VSC - GFOL with $\tau_{pq} = 1.1$

3.3.1 Analysis of the stable system with 2 VSC -GFOL

The Fig.29 below shows a closer view of the stable system with 2 VSC implemented. It can be observed that all the Eigenvalues are settled in the left half plane.

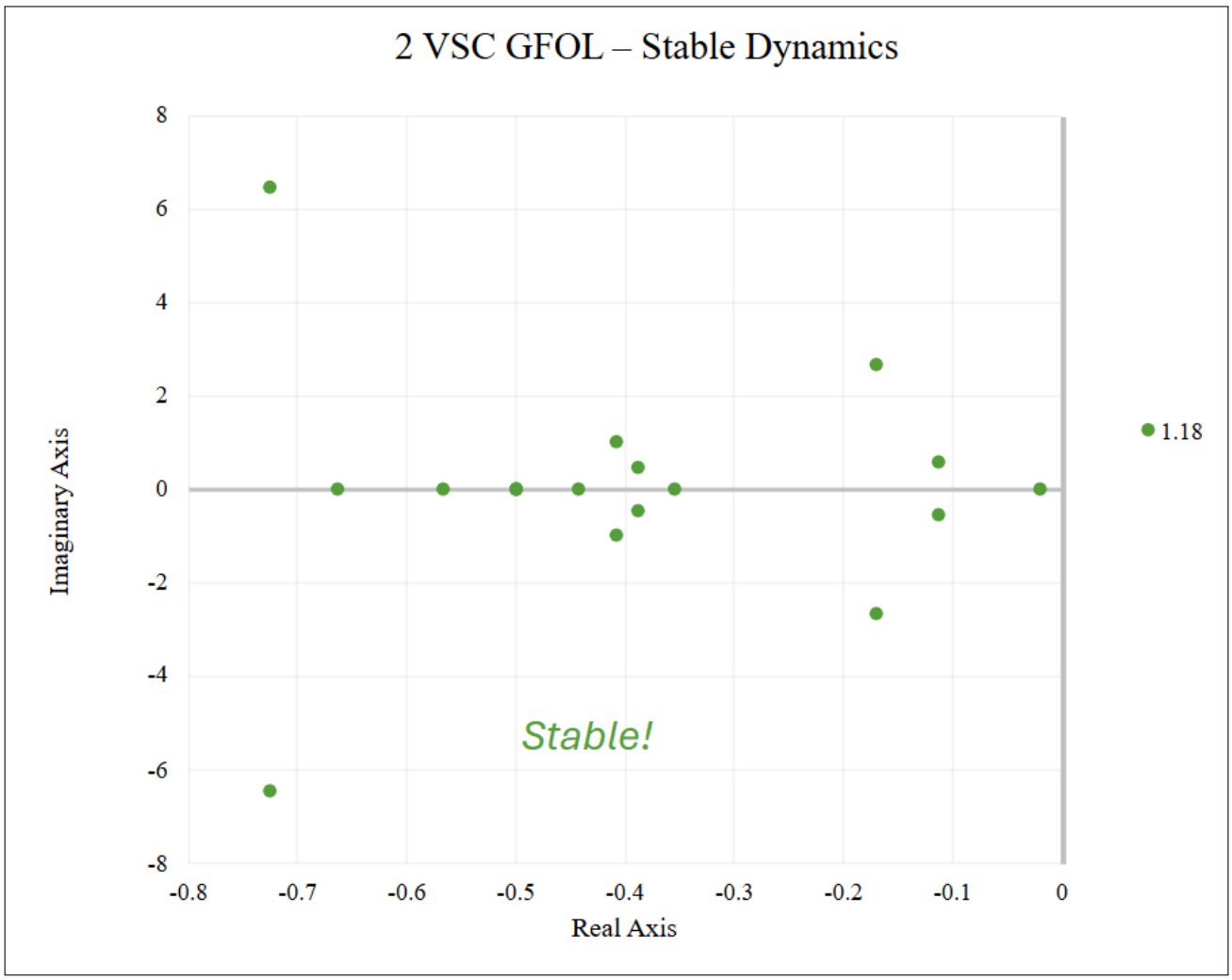

Figure 29: Eigenvalue movements (zoomed-in) for stable system with 2 VSC - GFOL for τ_{pq} = 1.18

From the Fig.30 below, it can be observed that the integration of the 2 VSCs increased the dynamics of the system. The system contains more of high frequency modes which were caused by the interactions of the VSC's controllers and capacitor. This is due to high frequency switching dynamics which the converters exhibit. Furthermore, the mode 4 and 5 with lower frequency was mainly an inter-area interaction between the two SG2 and SG3. This low frequency, low damped oscillation between areas may have tendencies of escalating small disturbance rapidly through out the entire system. Therefore, mechanism such as PSS, AVR, and POD for mitigating this interactions have to be properly tuned in order to damp out the oscillations within the machines.

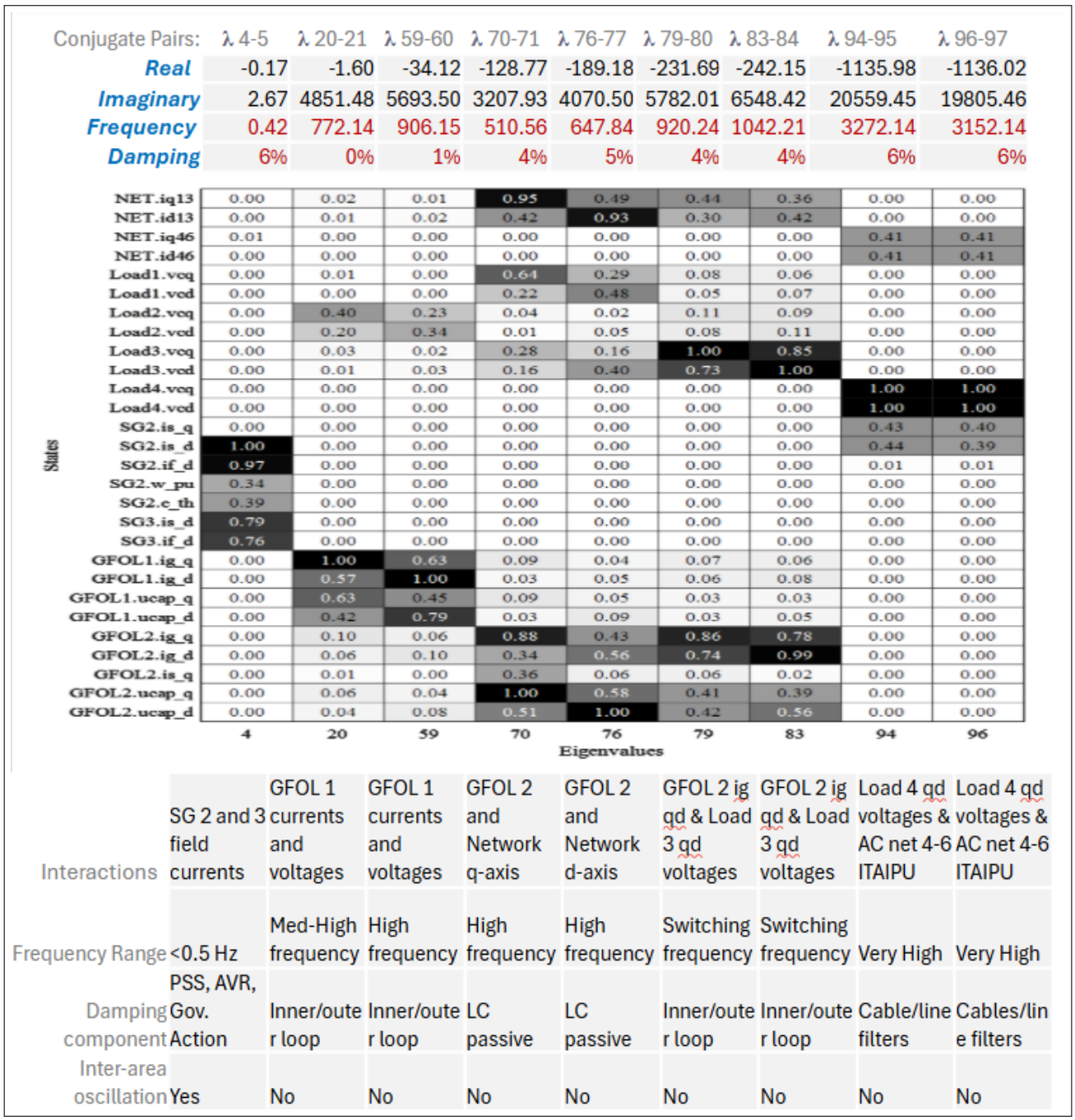

Figure 30: Reduced Participation Factor Matrix and Modal analysis for stable mode with 2 VSC - GFOL with $\tau_{pq} = 1.18$

4 Conclusion and Recommendations

4.1 Conclusion

Throughout this study, we have seen that replacing even a single synchronous machine with a grid-following converter disrupts the traditional small-signal stability of the hydro-dominated 7-bus network in two fundamental ways. First, the converter's lack of physical inertia removes the kinetic energy that dampens low-frequency swings, causing existing electromechanical modes, those inter-machine/ inter-area oscillations around 0.2 – 2Hz to become more lightly damped and, in some cases, unstable. Second, the converter control architecture itself introduces entirely new modes at much higher frequencies, tied to its filter dynamics, switching actions, and current loop interactions. Our eigenvalue analyses showed six such problematic modes emerge with a single converter substitution; removing two generators and inserting two converters amplified both effects, and pushing additional eigenvalues into the right half-plane.

Attempts to remove these instabilities by simply increasing inner-loop current-controller gains proved largely insufficient: the converter's internal dynamics and external network interactions limit the degree to which faster current tracking can add damping. Instead, our work demonstrated that modest retuning of the outer active power loop specifically, varying the power loop time constant τ_{pq} successfully reintroduced damping across all critical modes. This adjustment slows the converter's power response just enough to emulate inertia and absorb energy from both low and high frequency oscillations, shifting every unstable or marginal eigenvalue back into the left half plane.

From a practical standpoint, these results carry three key messages for system operators and converter manufacturers. First, it is insufficient to simply match nominal power ratings when integrating converters; control loop design must explicitly target system level stability across both conventional low frequency modes and converter driven high frequency resonances. Second, inertia emulation schemes should not be confined to a fixed P–f droop but must include adjustable power loop dynamics that can flexibly trade response speed for damping as system inertia changes. Third, because every converter adds its own suite of resonant modes, planners should maintain a minimum level of natural inertia or deploy grid forming converters with inherent stiffness to preserve phase angle separation and prevent coupling of critical modes.

Looking ahead, our study suggests several avenues for further work. Adaptive τ_{pq} tuning algorithms could dynamically optimize damping in real time as generation mixes shift or contingencies occur. Hybrid converter control architectures—capable of seamlessly switching between grid-forming and grid-following roles—might offer the best of both worlds by injecting inertia when needed and tracking power set-points otherwise. Finally, coordinated multi-device damping controllers, possibly implemented in a distributed fashion, could manage interactions among converters and remaining synchronous machines to enforce global stability objectives. By combining modal analysis tools like STAMP with real-time measurements and adaptive control

techniques, future power systems can accommodate high levels of renewable and converter-based penetration without sacrificing the robust stability we have long relied on.

4.2 Recommendations

To ensure robust stability in low inertia power systems with high penetration of IBR, the following could be considered:

- **Maintaining minimum inertia:** Keeping one or two synchronous machines online or deploying grid forming converters to preserve kinetic energy and prevent mode collapse.
- **Adaptive power loop tuning:** Automatically adjusting the VSC active power time constant (τ_{pq}) so damping scales with changing generation mixes and system conditions.
- **Hybrid control architectures:** Use converters that can switch between grid forming and grid following modes, offering both inertia support and precise power tracking.
- **Distributed damping controllers:** Coordinate virtual impedance loops, power oscillation damping filters, or control signals across devices to suppress low and high frequency oscillations.
- **Automated stability monitoring:** Leverage tools like STAMP with real time measurements and modal/impedance analysis to detect and address emerging risks before they threaten system stability.

4.3 Team members contribution

- **Joseph:** Simulation of the different cases using STAMP Tool, troubleshooting and debugging errors, analysis of the results and presentation. Report drafting, organization and reviews.
- **Stephanie:** Simulation of the different cases using STAMP Tool, debugging the codes, analysis and definition of scope of work, analysis of the results and presentation, workflow defined, eigenvalue movement data treatment. Report drafting, organization and reviews.

References

[1] IRENA, "Renewable energy roadmap for central america towards a regional energy transition," in *International Renewable Energy Agency, Abu Dhabi*, 2022.

[2] P. Kundur, "Power system stability and control," in *McGraw-Hill Education*, 1994.

[3] IEA, "Brazilian energy mix 2023," in *International Energy Agency*, 2024.

[4] L. Lima Dinemayer Silva and I. P. T. F. on Benchmark Systems for Stability Controls, "Report on the Benchmark System #2: 7-bus, 5-machine Equivalent Brazilian System," IEEE Power & Energy Society, Tech. Rep., version 3, Jul. 2015, Downloaded from IEEE PES Resource Center. [Online]. Available: https://resourcecenter.ieee-pes.org/publications/technical-reports/pestr18.

[5] CITCEA-UPC, "Stamp toolbox: A matlab-based toolbox for automated emt modelling and small-signal stability analysis of power systems," in *CITCEA-UPC Internal Report*, Available online, 2023.

[6] C. Collados-Rodriguez, M. Cheah-Mane, E. Prieto-Araujo, and O. Gomis-Bellmunt, "Stability and operation limits of power systems with high penetration of power electronics," in *Proceedings of the International Conference on Electrical Power and Energy Systems (IJEPES)*, vol. 138, 2022, p. 107 728. DOI: 10.1016/j.ijepes.2021.107728.

[7] C. Collados-Rodriguez, M. Cheah-Mane, E. Prieto-Araujo, and O. Gomis-Bellmunt, "Stability analysis of systems with high vsc penetration: Where is the limit?" *IEEE Transactions on Power Delivery*, vol. 35, no. 4, pp. 2021–2031, 2020. DOI: 10.1109/TPWRD.2019.2959541.